Journal of Power Sources 195 (2010) 7246–7249

Contents lists available at ScienceDirect

Journal of Power Sources

journal homepage: www.elsevier.com/locate/jpowsour

Short communication

An ambient aqueous synthesis for highly dispersed and active Pd/C catalyst for formic acid electro-oxidation

Niancai Cheng[a,b], Haifeng Lv[a], Wei Wang[a], Shichun Mu[a,*], Mu Pan[a], Frank Marken[b,**]

[a] State Key Laboratory of Advanced Technology for Materials Synthesis and Processing, Wuhan University of Technology, 430070, People's Republic of China
[b] Department of Chemistry, University of Bath, Claverton Down, Bath BA2 7AY, UK

ARTICLE INFO

Article history:
Received 30 April 2010
Accepted 22 May 2010
Available online 31 May 2010

Keywords:
Voltammetry
Pd nanoparticles
Formic acid oxidation
Ammonia complex
Fuel cell

ABSTRACT

An experimentally simple process is reported in aqueous solution and under ambient conditions to prepare highly dispersed and active Pd/C catalyst without the use of a stabilizing agent. The $[Pd(NH_3)_4]^{2+}$ ion is synthesized with gentle heating in aqueous ammonia solution without formation of $Pd(OH)_x$ complex intermediates. The adsorbed $[Pd(NH_3)_4]^{2+}$ on the surface of carbon (Vulcan XC-72) is reduced in situ to Pd nanoparticles by $NaBH_4$. The Pd/C catalyst obtained is characterized by X-ray diffraction (XRD) and transmission electron microscopy (TEM). The results show that highly dispersed Pd/C catalyst with 20 wt.% Pd content and with an average Pd nanoparticle diameter of 4.3–4.7 nm could be obtained. The electrochemical measurements show that the Pd/C catalyst without stabilizer has a higher electro-oxidation activity for formic acid compared to that of a Pd/C catalyst prepared in a traditional high temperature polyol process in ethylene glycol.

1. Introduction

Over the past decade, the direct formic acid fuel cells (DFAFCs) have attracted attention because of some advantages over the direct methanol fuel cell (DMFC) [1,2], which makes the DFAFC a promising candidate for power source applications in portable electronic devices. Formic acid exhibits lower fuel crossover through the polymer membrane and lower toxicity than methanol [3]. The electro-oxidation of formic acid commences at a less positive potential than methanol electro-oxidation [4].

Recent progress in formic acid electro-oxidation has revealed that the Pd-based catalyst has higher catalytic activity than Pt-based catalysts [5]. Studies have shown that the Pd electro-oxidation activity for formic acid is strongly influenced by the morphology and size of the Pd nanoparticles [6–10]. To control the Pd particles size and dispersion, surfactant agents or stabilizing polymer molecules such as RNA [11] or poly-vinylpyrrolidone (PVP) [12] have been employed during synthesis. Unfortunately, these stabilizers are usually strongly adsorbed onto the surface of Pd nanoparticles, which then may limit the catalytic activity because of blocking of "clean" and surface active sites [13]. Pd(II) is one of the readily hydrolysable metals and highly insoluble hydroxides ($Pd(OH)_x$) are usually formed in alkaline solution. Li et al. [14,15] prepared $[Pd(NH_3)_4]^{2+}$ using NH_3 in ethylene glycol under hydrothermal conditions to avoid the precipitation of $Pd(OH)_x$. Although a well-dispersed Pd/C catalyst was synthesized using this methodology, it was also difficult to purify with ethylene glycol strongly adsorbing onto the Pd nanoparticle surfaces. A large amount of $[Pd(NH_3)_4]^{2+}$ was adsorbed on the surface of carbon and then needed to be reduced in a H_2 atmosphere. This was required because ethylene glycol was not a sufficiently strong reducing agent for the $[Pd(NH_3)_4]^{2+}$ complex [14]. Here we report that an experimentally simple method to synthesize well-dispersed Pd/C catalyst using only gentle heating, no ethylene glycol, no stabilizer, and a short reaction time. The process employs aqueous NH_3 to avoid the precipitation of $Pd(OH)_x$ and a room temperature reduction with borohydride, hence avoiding the agglomeration and ripening of Pd nanoparticles.

2. Experimental

2.1. Chemical reagents

Palladium(II)chloride (>99.9%), hydrochloric acid, sodium borohydride and sulphuric acid were obtained from Shanghai Regent. Vulcan XC-72 carbon black (BET surface area = 250 $m^2\,g^{-1}$) was obtained from Cabot Corporation. Formic acid, ammonia, sodium hydroxide were obtained from Sigma–Aldrich. Demineralized and

* Corresponding author at: State Key Laboratory of Advanced Technology for Materials Synthesis and Processing, Wuhan University of Technology, 122 Luoshi Road, Wuhan, Hubei 430070, People's Republic of China.
Tel.: +86 0 27 87651837x8611; fax: +86 0 27 87879468.
** Corresponding author at: Department of Chemistry, University of Bath, Claverton Down, Bath BA2 7AY, UK. Tel.: +44 01225 383694; fax: +44 01225 386231.
E-mail addresses: msc@whut.edu.cn (S. Mu), f.marken@bath.ac.uk (F. Marken).

0378-7753/$ – see front matter © 2010 Elsevier B.V. All rights reserved.
doi:10.1016/j.jpowsour.2010.05.039

filtered water was taken from a AIKE Ultra-low Organics Lab water purification systems with a resistivity of not less than 18 MΩ cm.

2.2. Synthesis of carbon-supported Pd catalysts

First, 100 mg $PdCl_2$ was dissolved in 50 cm^3 water by the addition of 1 cm^3 aqueous HCl (1 mol dm^{-3}) at room temperature with vigorous stirring. Then, 1 cm^3 aqueous ammonia (37%, V/V) was added to the $PdCl_2$ solution and the color of the solution changed from yellow to pink, which indicates some intermediate formation of Pd(OH)x. The pink solution was then heated gently for ca. 3 min and the color of the solution changed from pink to colorless. After drop-wise addition of 1 mol dm^{-3} NaOH solution to adjust to pH 10, the XC-72 carbon was added to the solution and the slurry was stirred for 2 h. Next, $NaBH_4$ (0.5 cm^3 of 1 mol dm^{-3} in water) was added drop-wise into the stirred solution to reduce the $[Pd(NH_3)_4]^{2+}$ complex to Pd metal in situ. The slurry was stirred for another 4 h. After filtration, washing, and drying at 373 K in a vacuum oven, a 20 wt.% Pd/C catalyst was obtained. For comparison, a traditional 20 wt.% Pd/C catalyst was prepared following a literature method [16]. First, 1.5 cm^3 of an aqueous solution of 0.05 mol dm^{-3} $PdCl_2$ was mixed with 35 cm^3 of ethylene glycol in a 100 cm^3 beaker. Then 0.4 mol dm^{-3} KOH was added drop-wise to give a total volume of 37 cm^3 and the XC-72 carbon was added to the mixture and dispersed by sonication. The mixture was heated in a household microwave oven (Glaz P70D20TJ-D3, 2450 MHz, 700 W) for 50 s. The resulting suspension was filtered and the residue was washed and dried at 373 K in a vacuum oven.

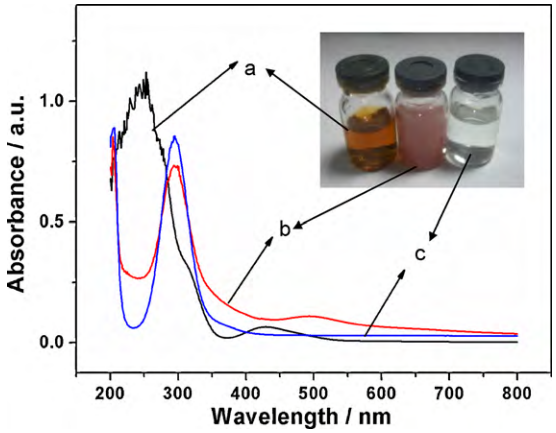

Fig. 1. UV/vis absorption spectra of aqueous solution of (a) 14 mM $[PdCl_4]^{2-}$, (b) 14 mM $[PdCl_4]^{2-}$ with aqueous ammonia before, and (c) after heating.

2.3. Characterization of carbon-supported catalysts

The electrochemical oxidation of formic acid was characterized with a three-electrode cell and computer controlled potentiostat system (PGSTAT12, AUTOLAB Electrochemical System). Working electrodes were prepared from 3 mm diameter glassy carbon disc electrodes. The catalyst powders were mixed with deionized water and 5 wt.% Nafion solution, and then coated on a mirror-polished glassy carbon disk electrode. Each working electrode contained ca. 40 μg cm^{-2} Pd catalyst. A saturated calomel electrode (SCE) was

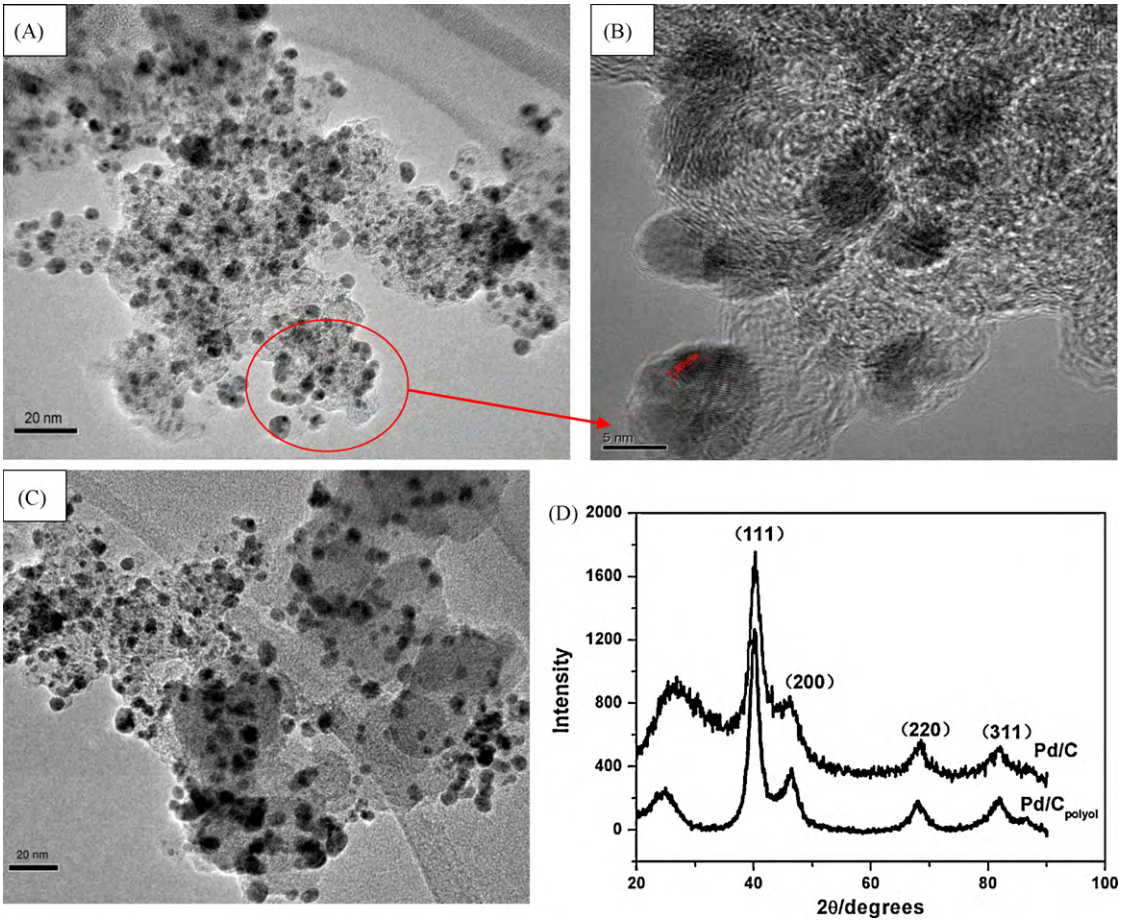

Fig. 2. Transmission electron microscope (TEM) images with low magnification (A) and high magnification (B) of the new Pd/C catalyst. (C) TEM image of the Pd/C catalyst produced with ethylene glycol. (D) XRD comparison of the new Pd/C catalyst and the Pd/C_{polyol} catalyst produced with ethylene glycol.

used as the reference electrode, and a platinum wire served as the counter electrode. Cyclic voltammetry experiments were carried out in 0.5 M H_2SO_4. Electrochemical formic acid oxidation activity testing was carried out in 0.5 M H_2SO_4 + 0.5 M HCOOH solution. The above measurements were carried out at room temperature (293 ± 2 K).

Morphology analysis of the newly prepared catalyst was performed with a JEOL 2010 high-resolution transmission electron microscope (HRTEM). Powder XRD measurements were performed on a Ragaku D/MAX-IIA X-ray diffractometer using Cu-Kα radiation. The UV–vis absorption spectrum of the resulting catalysts was measured with a Perkin-Elmer Model lambda17 recording spectrophotometer.

3. Results and discussion

The aqueous solution containing $[PdCl_4]^{2-}$ ions is yellow and shows two characteristic peaks in UV–vis absorption spectra at ca. 235 nm and 428 nm due to the ligand-to-metal charge-transfer transitions [17] (Fig. 1). After addition of aqueous NH_3 to the solution, the color turns from yellow to pink and the adsorption peaks were shifted to 295 nm and 490 nm, respectively. The adsorption peak at 295 nm can be attributed to $[Pd(NH_3)_4]^{2+}$ ions, whereas the peak at 490 nm indicates formation of $Pd(OH)_x$ [18]. After the solution is gently heated, the color of the solution and an adsorption peak at 490 nm disappear and the peak at 295 nm increases, suggesting that the $Pd(OH)_x$ complex is converted into $[Pd(NH_3)_4]^{2+}$ ions.

Fig. 2A–C shows TEM images for the new Pd/C catalyst and for Pd/C_{polyol} catalyst. The Pd nanoparticles for both catalysts are fully dispersed in the carbon support. The average sizes of Pd nanoparticles are estimated as 4.7 nm for Pd/C catalyst and 5.2 nm for Pd/C_{polyol} catalyst based on the corresponding distribution histogram (not shown). The crystal domains within each Pd nanoparticle have an inter-fringe distance of 0.22 nm (Fig. 2B), which is close to the lattice spacing of the (1 1 1) planes of the face-centered cubic (fcc) Pd crystal (0.223 nm). The crystal structure of Pd/C and Pd/C_{polyol} catalysts are determined by power X-ray diffraction (see Fig. 2D). There are four observed characteristic diffraction peaks at ca. 40°, 46°, 68° and 82° belonging to the face-centered cubic (fcc) phase of Pd and the (1 1 1) plane has the largest intensity among those plane. Based on Fig. 2, the Pd catalysts mainly exhibit the (1 1 1) plane. The (1 1 1)-faced Pd catalyst is more practical for fuel cell application [13] because the (1 1 1) planes are less susceptible to oxidation [19]. The peaks for the Pd/C catalyst are slightly broader than those for the Pd/C_{polyol} catalyst. The average sizes of the Pd nanoparticles are 4.3 nm for Pd/C catalyst and 4.9 nm for Pd/C_{polyol} catalyst when calculated with the Scherrer formula [20,21] in good agreement with the values measured from the TEM image in Fig. 2A and 2C. Recent studies show that carbon-supported Pd nanoparticles of 4–7 nm diameters are favorable in practical applications in DFAFCs [10,22].

Fig. 3A shows a comparison of cyclic voltammetry data for the Pd/C and Pd/C_{polyol} catalysts immersed in 0.5 M H_2SO_4 at the scan rate of 50 mV s^{-1}. The sharp peak observed for the Pd/C catalyst in the hydrogen adsorption/desorption region is attributed to the oxidation of the adsorbed hydrogen on Pd. The electrochemical surface area (ECSA) for Pd/C catalyst as obtained from cyclic voltammetry data (based on the charge under the hydrogen desorption peaks) is 56 m^2 g^{-1}, which is larger than the ECSA (44 m^2 g^{-1}) for Pd/C_{polyol} catalyst. This is in accord with the results of XRD and TEM described above. These results are also supported by the electrochemical behavior in the Pd oxidation/reduction region. The observed difference in current density of can be ascribed mainly to the difference in surface areas and only to an insignificant extent to the presence

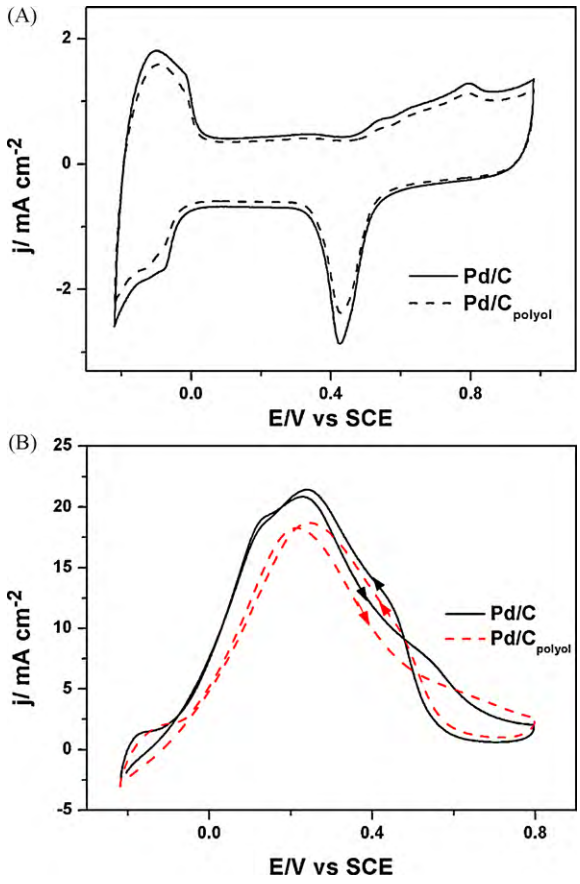

Fig. 3. (A) Cyclic voltammetry (CV) data for the Pd/C and Pd/C_{polyol} catalysts immersed in 0.5 M H_2SO_4 at the scan rate of 50 mV s^{-1}. (B) Cyclic voltammograms for Pd/C and Pd/C_{polyol} catalysts immersed in 0.5 M H_2SO_4 + 0.5 M formic acid at a scan rate of 50 mV s^{-1}. The working electrode in these experiments contained ca. 40 μg cm^{-2} catalyst.

of ethylene glycol residues. Fig. 3B shows the electro-oxidation activity for formic acid on both Pd/C and Pd/C_{polyol} catalysts. The Pd/C catalyst exhibits a higher activity of formic acid oxidation compared to the Pd/C_{polyol} catalyst which is mainly due to the smaller nanoparticle size of Pd/C catalyst. The peak current density of Pd/C catalyst is 20.74 mA cm^{-2} and that of Pd/C_{polyol} catalyst is 18.24 mA cm^{-2} at the positive-going potential scans. The peak current densities are 21.50 mA cm^{-2} and 18.53 mA cm^{-2} for Pd/C catalyst and Pd/C_{polyol} catalysts, respectively, for the negative-going potential scans. The overall mechanism tentatively proposed for formic acid electro-oxidation to CO_2 at nanoparticle catalysts is based on a triple pathway process [23,24]. A "direct pathway" involving a formate anion possibly bound to Pd via CH-activation has been suggested to occur during facile oxidation directly to CO_2 (Eq. (1)). A second process termed "formate pathway" involves formate bound via oxygen (bound via OH-activation) may require a substantially higher activation energy for the conversion into CO_2 and is therefore considered inefficient (Eq. (2)).

$$Pd + HCOOH \rightarrow Pd\text{-}COOH^- + H^+ \rightarrow Pd + CO_2 + 2H^+ + 2e^- \quad (1)$$

$$Pd + HCOOH \rightarrow Pd\text{-}O_2CH^- + H^+ \rightarrow Pd + CO_2 + 2H^+ + 2e^- \quad (2)$$

A third "indirect pathway" based on a aestivating intermediate may occur in particular under dehydrating conditions where the adsorption of CO (formed by interfacial dehydrogenation of HCOOH) is causing "blocking" of the catalyst surface and an additional over potential for CO_2 formation (Eq. (3)).

$$Pd + HCOOH \rightarrow Pd\text{-}CO + H_2O \rightarrow Pd + CO_2 + 2H^+ + 2e^- \quad (3)$$

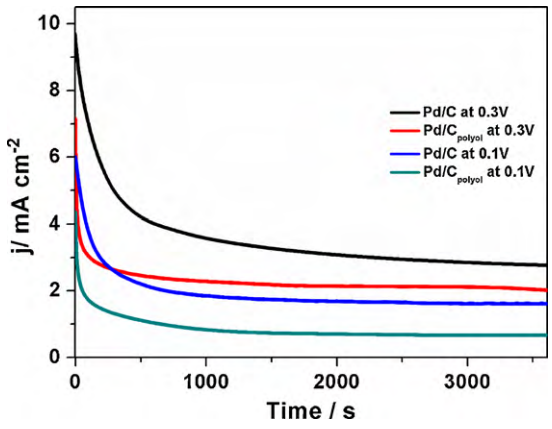

Fig. 4. Chronoamperometric data for Pd/C and Pd/C_{polyol} catalysts immersed in 0.5 M H_2SO_4 + 0.5 M formic acid at 0.1 V and 0.3 V vs. SCE.

Based on the slight change of the peak current density at positive going vs. negative-going potential scans, we speculate that the formic acid oxidation on Pd catalyst formic acid oxidation here mainly occurs through "direct pathway". If the formic acid was mainly oxidized to CO_2 by the "indirect pathway", the peak current density at negative-going potential scan should larger than that at positive-going potential scan because CO adsorbed on the nanoparticle can be oxidized to CO_2 at higher potential, not lower potential [25].

Chronoamperometry curves for formic acid electro-oxidation on both Pd/C and Pd/C_{polyol} catalysts are shown in Fig. 4. It is obvious that the steady-state current density for the Pd/C catalyst is larger than that for the Pd/C_{polyol} catalyst. At 0.1 V vs. SCE, the steady-state current density for the Pd/C catalyst (1.6 mA cm^{-2}) is typically about twice larger than that observed for the Pd/C_{polyol} catalyst (0.8 mA cm^{-2}). At 0.3 V vs. SCE, the steady-state current density for the Pd/C catalyst is 2.8 mA cm^{-2} which is ca. 1.4 times higher than that of Pd/C_{polyol} catalyst (1.8 mA cm^{-2})

4. Conclusion

We report an experimentally simple and effective method to prepare a highly dispersed and active Pd/C catalyst without any stabilizing agent and employing ambient aqueous conditions for conversion of $Pd(OH)_x$ to $[Pd(NH_3)_4]^{2+}$ and the reduction to Pd metal. Reduction is carried out in situ in aqueous $NaBH_4$. The resulting Pd nanoparticles on the Vulcan XC-72 carbon support are ca. 4.3–4.7 nm in diameter with a diffraction pattern for the Pd face-centered cubic (fcc) crystal structure and (1 1 1) the dominating crystal face. Cyclic voltammetry and chronoamperometry tests indicate a better formic acid electro-oxidation activity for the Pd/C catalyst compared to that for Pd/C_{polyol} catalyst prepared by a traditional method. For catalyst optimization, further work will be required to study the effect of pH and the reducing agent on the Pd size and dispersion as well as the performance and durability of the catalyst under DFAFC conditions.

Acknowledgements

This work was supported by the National Science Foundation of China (50972112 and 50632050) and the New Century Excellent Talent Program of Ministry of Education of China (NCET-07-0652).

References

[1] M.D. Obradovic, A.V. Tripkovic, S.L. Gojkovic, Electrochim. Acta 55 (2009) 204–209.
[2] L. Zhang, T. Lu, J. Bao, Y. Tang, C. Li, Electrochem. Commun. 8 (2006) 1625–1627.
[3] X. Wang, J.M. Hu, I.M. Hsing, J. Electroanal. Chem. 562 (2004) 73–80.
[4] J. Willsau, J. Heitbaum, Electrochim. Acta 31 (1986) 943–948.
[5] X. Yu, P.G. Pickup, J. Power Sources 182 (2008) 124–132.
[6] W.P. Zhou, A. Lewera, R. Larsen, R.I. Masel, P.S. Bagus, A. Wieckowski, J. Phys. Chem. B 110 (2006) 13393–13398.
[7] H. Meng, S. Sun, J.-P. Masse, J.-P. Dodelet, Chem. Mater. 20 (2008) 6998–7002.
[8] H. Lee, S.E. Habas, G.A. Somorjai, P. Yang, J. Am. Chem. Soc. 130 (2008) 5406–5407.
[9] R.K. Pandey, V. Lakshminarayanan, J. Phys. Chem. C 113 (2009) 21596–21603.
[10] W. Zhou, J.Y. Lee, J. Phys. Chem. C 112 (2008) 3789–3793.
[11] L.A. Gugliotti, D.L. Feldheim, B.E. Eaton, Science 304 (2004) 850–852.
[12] Y. Xiong, J. Chen, B. Wiley, Y. Xia, J. Am. Chem. Soc. 127 (2005) 7332–7333.
[13] V. Mazumder, S. Sun, J. Am. Chem. Soc. 131 (2009) 4588–4589.
[14] H. Li, G. Sun, Q. Jiang, M. Zhu, S. Sun, Q. Xin, J. Power Sources 172 (2007) 641–649.
[15] H. Li, G. Sun, Q. Jiang, M. Zhu, S. Sun, Q. Xin, Electrochem. Commun. 9 (2007) 1410–1415.
[16] Z. Liu, L. Hong, M.P. Tham, T.H. Lim, H. Jiang, J. Power Sources 161 (2006) 831–835.
[17] T. Teranishi, M. Miyake, Chem. Mater. 10 (1998) 594–600.
[18] T. Lopez, M. Villa, R. Gomez, J. Phys. Chem. 95 (1991) 1690–1693.
[19] M. Baldauf, D.M. Kolb, J. Phys. Chem. 100 (1996) 11375–11381.
[20] E. Antolini, F. Cardellini, J. Alloys Compd. 315 (2001) 118–122.
[21] V. Radmilovic, H.A. Gasteiger, P.N. Ross, J. Catal. 154 (1998) 98–106.
[22] Y. Zhu, Y.Y. Kang, Z.Q. Zou, Q. Zhou, J.W. Zheng, B.J. Xia, H. Yang, Electrochem. Commun. 10 (2008) 802–805.
[23] Y.X. Chen, M. Heinen, Z. Jusys, R.J. Behm, Angew. Chem. 45 (2006) 981–985.
[24] M. Neurock, M. Janik, A. Wieckowski, Faraday Discuss. 140 (2008) 363–378.
[25] J.L. Cohen, D.J. Volpe, H.D. Abruña, Phys. Chem. Chem. Phys. 9 (2007) 49–77.